

A unique case of childhood hypophosphatasia caused by a novel heterozygous 51-bp in-frame deletion in the *ALPL* gene

Kanako Tachikawa¹, Miwa Yamazaki¹, and Toshimi Michigami¹

¹Department of Bone and Mineral Research, Research Institute, Osaka Women's and Children's Hospital, Osaka Prefectural Hospital Organization, Osaka, Japan

Highlights

- Clinical manifestation of childhood hypophosphatasia is highly variable.
- A novel 51-bp deletion in *ALPL* was identified in a case of hypophosphatasia.
- The variant protein was suggested to have a dominant-negative effect.

Abstract. Hypophosphatasia (HPP) is caused by inactivating variants of the *ALPL* gene, which encodes tissue non-specific alkaline phosphatase (TNSALP). Among the six subtypes of HPP, childhood HPP presents after 6 months and before 18 yr of age, and is inherited in both autosomal dominant and autosomal recessive manners. Patients with childhood HPP have variable symptoms, including rickets-like bone changes, low bone mineral density (BMD), short stature, muscle weakness, craniosynostosis, and premature loss of deciduous teeth. Here, we describe a 7-yr-old boy with childhood HPP who showed short stature, impaired ossification of the carpal bones, and low BMD. Genetic testing identified a novel heterozygous 51-bp in-frame deletion in the *ALPL* gene (c.1482_1532del51), leading to the lack of 17 amino acids between Gly495 and Leu511 (p.Gly495_Leu511del). *In vitro* transfection experiments revealed the loss of enzymatic activity and the dominant-negative effect of the TNSALP[p.Gly495_Leu511del] variant; thus, the patient was diagnosed as having autosomal dominant HPP. The TNSALP[p.Gly495_Leu511del] variant was localized to the plasma membrane as was the wild-type TNSALP (TNSALP[WT]); however, co-immunoprecipitation experiments suggested a reduced dimerization between TNSALP[p.Gly495_Leu511del] and TNSALP[WT]. This case expands the variable clinical manifestation of childhood HPP and sheds light on the molecular bases underlying the dominant-negative effects of some TNSALP variants.

Key words: hypophosphatasia, *ALPL*, deletion, mutation, dominant-negative effect

Received: March 13, 2023 Accepted: April 18, 2023 Advanced Epub: May 6, 2023

Corresponding author: Toshimi Michigami, M.D., Ph.D., Department of Bone and Mineral Research, Research Institute, Osaka Women's and Children's Hospital, Osaka Prefectural Hospital Organization, 840 Murodo-cho, Izumi, Osaka 594-1101, Japan

E-mail: michigami@wch.opho.jp



This is an open-access article distributed under the terms of the Creative Commons Attribution Non-Commercial No Derivatives (by-nc-nd) License <<http://creativecommons.org/licenses/by-nc-nd/4.0/>>.

Copyright© 2023 by The Japanese Society for Pediatric Endocrinology



Introduction

Hypophosphatasia (HPP) is an inherited disorder caused by inactivating variants of the *ALPL* gene that encodes tissue non-specific alkaline phosphatase (TNSALP) (1–3). TNSALP is an ectoenzyme located on the plasma membrane of osteoblasts that hydrolyzes its substrates, including inorganic pyrophosphate (PPi), to produce inorganic phosphate (Pi). Since PPi inhibits the formation and growth of hydroxyapatite, the inactivation of TNSALP in HPP leads to impaired skeletal mineralization. The vitamin B6 metabolite pyridoxal 5'-phosphate (PLP) also serves as a substrate for TNSALP, and patients with HPP can be associated with vitamin B6-dependent seizures (1).

HPP is characterized by impaired skeletal mineralization and dental problems such as the premature loss of deciduous teeth; however, the age of onset and clinical features of HPP are highly diverse. Hence, HPP is generally classified into six subtypes: perinatal severe, perinatal benign, infantile, childhood, adult, and odonto HPP (2, 3). Patients with perinatal severe HPP manifest symptoms during the fetal/neonatal period, which include severe hypomineralization of all bones, respiratory problems, and convulsions. The life prognosis of patients with perinatal severe HPP is very poor if left untreated. On the other hand, perinatal benign HPP is characterized by a deformity of the long bones and is detectable via fetal ultrasound. However, it presents a good life prognosis despite its perinatal onset. Symptoms in infantile HPP include the failure to thrive and hypercalcemia/hypercalciuria. Approximately half of the patients with this form of HPP died early from respiratory complications before the introduction of enzyme replacement therapy with asfotase alfa. Childhood HPP presents after 6 months of age, and the symptoms presented are highly variable. Patients with childhood HPP may show rickets-like bone changes, poor bone mineralization, low bone mineral density (BMD), short stature, muscle weakness, craniosynostosis, and premature loss of deciduous teeth. Adult HPP presents after 18 yr of age and may manifest as bone fragility, muscle weakness, and pseudogout. Patients with odonto HPP only have dental problems without skeletal manifestations (3).

HPP is usually transmitted in an autosomal recessive manner, but milder forms, such as childhood, adult, and odonto HPP can be inherited in both autosomal recessive and dominant manners (1–3). To date, more than 400 *ALPL* variants have been identified to be responsible for HPP and are summarized in the *ALPL* Gene Variant Database (<https://alplmutationdatabase.jku.at/>). Here we describe a unique case of childhood HPP in whom a novel heterozygous 51-bp in-frame deletion in the *ALPL* gene (c.1482_1532del51) was identified. This deletion resulted in the loss of 17 amino acids between glycine at codon 495 and leucine at codon 511 (p.Gly495_Leu511del). *In vitro* transfection experiments using plasmids carrying wild-type (WT) and *ALPL* variants

demonstrated the loss of enzymatic activity and a dominant-negative effect of TNSALP[p.Gly495_511del].

Case Description

The patient was a boy born at the 39th gestational week between unrelated parents. His APGAR scores were 8 at 1 min and 9 at 5 min. His birth weight was 3,000 g (– 0.1 SD) and his height was 50.0 cm (+ 0.5 SD). At the age of 7 yr and 5 mo, he consulted a nearby hospital because of his short stature. His growth chart is shown in **Fig. 1A**. In his left wrist X-ray, only one carpal bone was observed, leading to a considerable delay in bone age (< 3.2 yr, TW2 method) (**Fig. 1B**). The radiolucency of his metacarpal bones was increased. His plasma IGF-1 level was 74 ng/mL (reference range: 63–247 ng/mL). Two GH provocation tests (arginine and L-dopa tests) were performed, one of which excluded complete GH deficiency. The peak GH value was 5.11 ng/mL in the arginine test, while it was 8.00 ng/mL in the L-dopa test. His thyroid function was normal. It was noticed that he had a low serum alkaline phosphatase (ALP) activity (260 U/L in the JSCC method; reference range: 450–1,250 U/L).

At the age of 7 yr and 9 mo, he was referred to our hospital for the investigation of possible HPP since his serum ALP activity was low after repeated measurements. His height was 109.8 cm (– 2.7 SD), and his body weight was 17.0 kg (– 3.0 SD). His body mass index (BMI) was 14.1, with a BMI-SDS of – 1.16. His father's height was 174 cm, and his mother's height was 153 cm. He did not have a history of either fractures or premature loss of deciduous teeth. He did not show lower limb deformities and had neither bone pain nor gait abnormalities. The BMD of his lumbar vertebrae (L2–L4) measured via dual-energy X-ray absorptiometry (DXA) using a Hologic Horizon A scanner was 0.382 g/cm², and its Z-score based on the densitometer-derived reference value was – 5.8. An X-ray of his spine demonstrated extremely radiolucent vertebral bodies, although obvious fractures were not found (**Fig. 1C**). His urinary phosphoethanolamine (PEA) level was 26.9 mmol/mol creatinine (237.9 μmol/g creatinine), which was elevated compared to the reference range reported by Imbard *et al.* (< 10 mmol/mol creatinine for 7 yr of age) (4). His serum calcium and phosphate levels were within normal ranges: 9.4 mg/dL and 5.2 mg/dL, respectively. His serum 25-hydroxyvitamin D level was 43.2 ng/mL, suggesting sufficient vitamin D status, and his serum intact parathyroid hormone level was normal (22 pg/mL).

The patient's father's serum ALP activity was low normal (157 U/L in the JSCC method; reference range: 130–350 U/L). The father had an avulsion fracture of the anterior cruciate ligament at the age of 14 years, and a rib fracture at the age of 16 yr. The patient's mother's serum ALP activity was 222 U/L in the JSCC method (reference range: 130–350 U/L).

The patient's bone mineralization defect, low BMD,

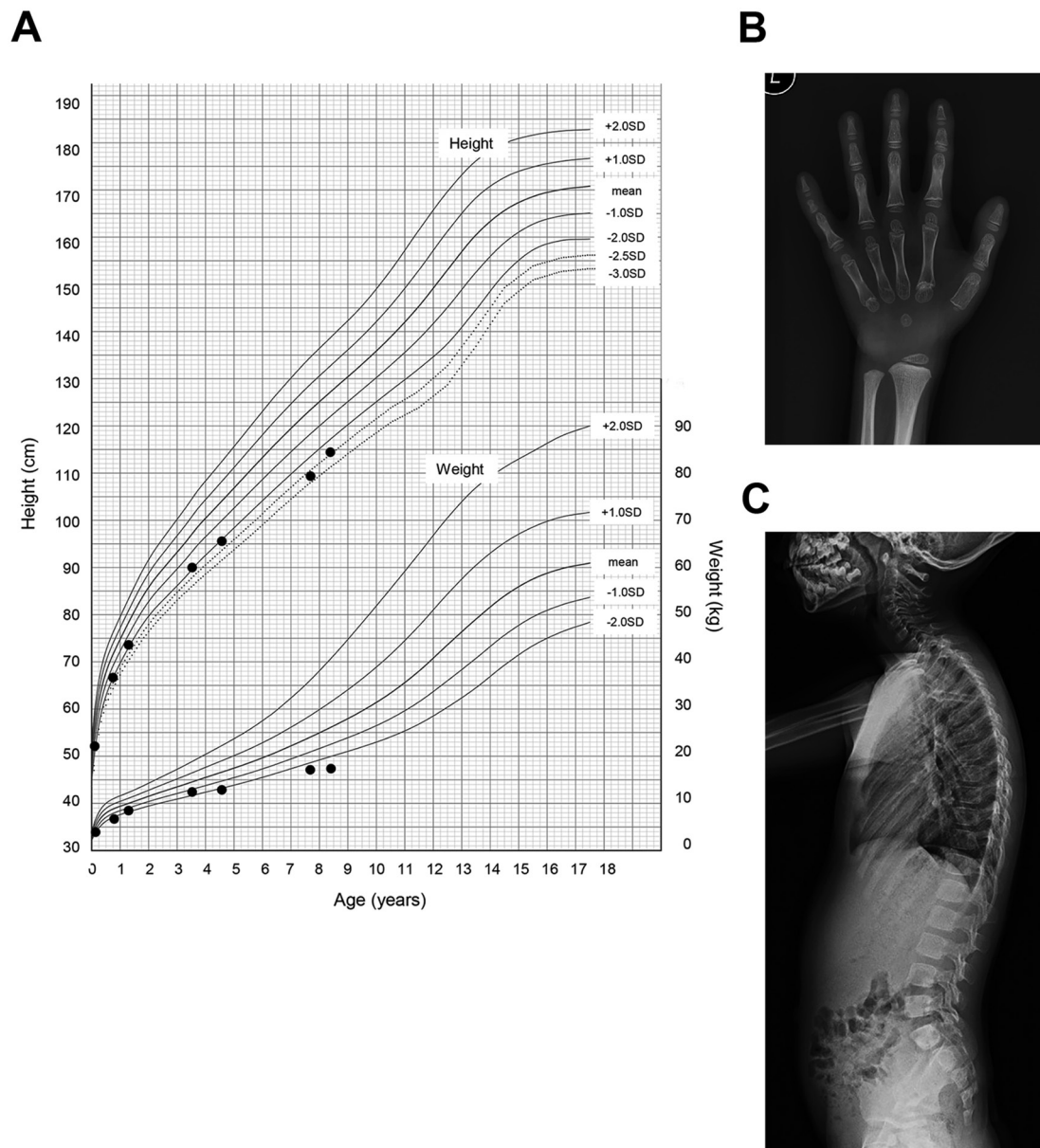


Fig. 1. The growth chart and radiologic findings in the patient. (A) The patient's growth chart was plotted on the standard growth curves of Japanese boys. (B) An X-ray of the patient's left wrist taken at the age of 7 yr and 5 mo. Impaired ossification of the carpal bones and increased radiolucency of the metacarpal bones were observed. (C) Highly radiolucent vertebral bodies in the patient's spinal X-ray. Obvious fractures were not found.

short stature, and consistently low levels of serum ALP activity suggested the diagnosis of HPP.

Methods

Ethical considerations

The study was approved by the institutional review board of Osaka Women's and Children's Hospital (approval number 776). Written informed consent was obtained from the parents of the patient.

Mutation analysis

Genomic DNA was extracted from peripheral blood leukocytes and subjected to polymerase chain reaction (PCR) to amplify the sequences corresponding to each coding exon of *ALPL* with exon/intron boundaries using the primers reported previously (5). The amplified fragments were then gel-purified and directly subjected to Sanger sequencing after being cloned into the pT7-Blue vector (Novagen, Madison, WI, USA).

Characterization of the variant TNSALP protein

The expression plasmids for green fluorescent protein (GFP)-tagged TNSALP (pcDNA-GFP-ALP) and FLAG-tagged TNSALP (pFLAG-ALP) were constructed as previously described (6, 7). Mutagenesis was performed using the QuikChange Lightning Site-Directed Mutagenesis Kit (Agilent Technologies, Palo Alto, CA, USA). The plasmids encoding GFP-tagged WT and variant TNSALP proteins were transfected into COS7 cells using the FuGENE HD Reagent (Roche Diagnostics, Indianapolis, IN, USA). We used expression plasmids encoding GFP-tagged vitamin D receptor (pGreenLantern-GFP and pSG5-VDR-GFP) as mock plasmids in some experiments.

Three days after transfection, cell lysates were harvested in 10 mM Tris-HCl buffer (pH 7.4) containing 0.05% Triton X-100 to determine TNSALP activity using *p*-nitrophenylphosphate (Sigma-Aldrich, St. Louis, MO, USA) as a substrate. Aliquots of the lysates were subjected to western blotting with an anti-GFP mouse monoclonal antibody (Roche Diagnostics, Mannheim, Germany) as the primary antibody, and densitometry of the signals was performed using ImageJ software.

The cytosolic and membrane fractions were also harvested from the transfected cells. Briefly, the cells were collected in ice-cold phosphate-buffered saline and subjected to three freeze-thaw cycles. Then, the lysates were centrifuged at $13,000 \times g$ for 25 min at 4°C, and the supernatants were collected as cytosolic fractions. Next, the pellets were resuspended in a membrane protein extraction buffer (20 mM Tris-HCl [pH 8.0], 150 mM NaCl, 1 mM EDTA, 1 mM EGTA, 1% Triton X-100). After three freeze-thaw cycles, the lysates were centrifuged at $13,000 \times g$ for 25 min at 4°C, and the supernatants were harvested as membrane fractions. The cytosolic and membrane fractions were then subjected to western blotting using anti-GFP, anti-integrin β 1 (Cell Signaling Technology, Beverly, MA, USA), and anti-GAPDH antibodies (Santa Cruz Biotechnology, Santa Cruz, CA, USA).

For co-immunoprecipitation experiments, cell lysates were harvested in a lysis buffer (10 mM Tris-HCl [pH 8.0], 150 mM NaCl, 5 mM EDTA, 0.5% Nonidet P-40, 10% glycerol) supplemented with a protease inhibitor cocktail (Complete™ EDTA-free; Roche Diagnostics). The cell lysates were incubated with anti-GFP mouse monoclonal antibodies, and the immunocomplex was immobilized on protein A/G agarose gel (Santa Cruz Biotechnology) at 4°C overnight. The immunoprecipitates were then extensively washed and subjected to western blotting using anti-GFP rabbit polyclonal antibody (Proteintech, Rosemont, IL, USA) and anti-FLAG rabbit polyclonal antibody (Rockland Immunochemicals, Gilbertsville, PA, USA).

Results

Identification of a heterozygous 51-bp in-frame deletion variant in the *ALPL* gene

We analyzed the *ALPL* gene of the patient to diagnose HPP and identified a heterozygous 51-bp in-frame deletion in exon 12 (c.1482_1532del51) (Fig. 2). This 51-bp in-frame deletion was suggested to result in the deletion of 17 amino acid residues between Gly495 and Leu511. The full-length WT TNSALP protein is composed of 524 amino acids, including the N-terminal signal peptide, whereas the TNSALP[p.Gly495_Leu511del] variant only consists of 507 amino acids. The identified deletion was also detected in one of the *ALPL* alleles of the patient's father.

Loss of enzymatic activity and dominant-negative effect of the TNSALP[p.Gly495_511del] variant

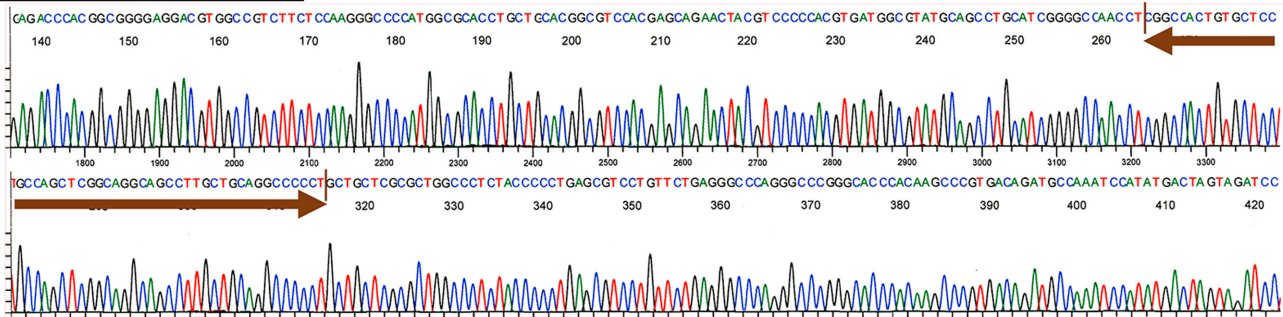
Next, we characterized the TNSALP[p.Gly495_Leu511del] variant using *in vitro* transfection experiments to confirm if the identified deletion indeed impaired the function of the TNSALP protein. GFP-tagged TNSALP proteins were exogenously expressed in COS7 cells, and their enzymatic activity in the cell lysates was determined using *p*-nitrophenylphosphate as a substrate. The expression plasmid for GFP-tagged VDR was used as a mock plasmid since its expression level in the transfected COS7 cells was similar to that of the GFP-tagged TNSALP proteins. Aliquots of the lysates were subjected to western blotting using anti-GFP antibodies, confirming the protein expression of both the WT and the variant GFP-tagged TNSALP proteins. When co-expressed, the signals of TNSALP[p.Gly495_Leu511del] and TNSALP[WT] were difficult to detect separately in the blot. The enzymatic activity of TNSALP was normalized based on the signal intensity of the GFP-tagged proteins. We found that TNSALP[p.Gly495_Leu511del] showed markedly reduced enzymatic activity compared to the TNSALP[WT]. Furthermore, co-transfection with TNSALP[p.Gly495_511del] suppressed the enzymatic activity of TNSALP[WT], suggesting its dominant-negative effect (Fig. 3A).

Localization of TNSALP[WT] and TNSALP[Gly495_511del] on the plasma membrane

TNSALP is an ectoenzyme localized on the cell plasma membrane (8). Thus, we next examined the subcellular distribution of the TNSALP[p.Gly495_Leu511del] variant by western blotting using the cytosolic and membrane fractions collected from the cells transfected with the GFP-tagged WT or variant TNSALP. Successful separation of the cytosolic and membrane fractions was verified by blotting with antibodies against GAPDH (a cytosolic protein) and

A

Wild-type allele



B

Variant allele

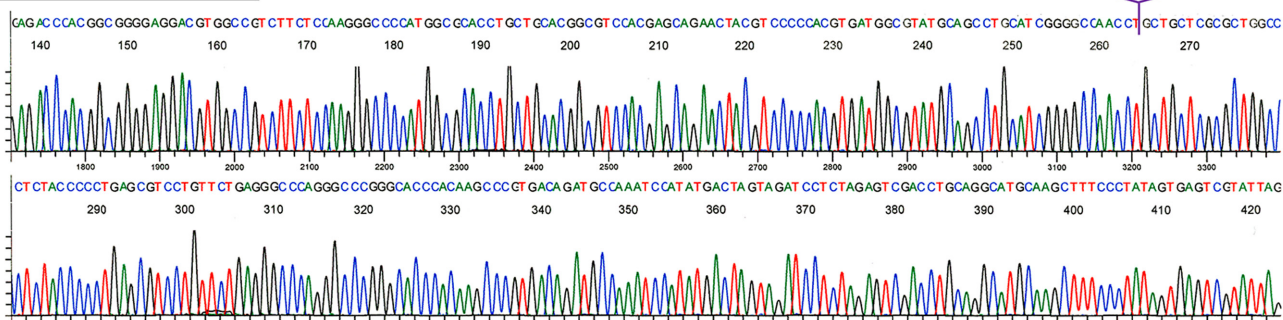


Fig. 2. Chromatograms of Sanger sequencing after TA cloning. Since direct sequencing of PCR products suggested a heterozygous deletion in exon 12, we performed Sanger sequencing after TA cloning. Representative partial sequences of the wild-type (A) and variant (B) alleles are shown. Among the nine clones sequenced, three were found to be the variant *ALPL* (c.1482_1532del51) shown in (B). The brown two-headed arrow in (A) indicates the 51-bp fragment, which is deleted in the variant allele as depicted by an inverted triangle in (B).

integrin $\beta 1$ (a membrane-associated protein). Both GFP-tagged TNSALP[WT] and TNSALP[p.Gly495_Leu511del] proteins were found to be localized on the plasma membrane (**Fig. 3B**).

Reduced dimer formation and/or stability between TNSALP[WT] and TNSALP[Gly495_511del]

Since TNSALP functions as a dimer, we next performed co-immunoprecipitation experiments to examine the dimerization between the WT and variant TNSALP proteins. We found that FLAG-tagged TNSALP[WT] was co-immunoprecipitated with GFP-tagged TNSALP[WT] but not with GFP-tagged VDR. Moreover, the co-immunoprecipitation of FLAG-tagged TNSALP[WT] was detected, but was markedly reduced for GFP-tagged TNSALP[p.Gly495_Leu511del] compared to that for GFP-tagged TNSALP[WT] (**Fig. 3C**). These results suggested an impaired dimer formation and/or stability of the TNSALP[p.Gly495_Leu511del] variant with the TNSALP[WT].

Discussion

HPP is usually classified into six subtypes based on the age of onset and clinical manifestations: namely, perinatal severe, perinatal benign, infantile, childhood, adult, and odonto HPP. We previously analyzed 98 Japanese patients with HPP and found that the perinatal severe HPP was the most frequent (45.9%) and the perinatal benign HPP was the second most frequent (22.4%) subtype (2). The high prevalence of two possible founder variants of *ALPL*, p.Leu520ArgfsX86 and p.Phe327Leu, may have caused the high frequency of the perinatal severe and perinatal benign HPP, respectively, in Japanese patients with HPP. On the other hand, childhood HPP, where the disease onset is after 6 months and before 18 years of age, appears less frequent in Japan than the perinatal forms (2).

Considering the age of onset, the current patient was classified as having childhood HPP. In addition to low serum ALP activity, he showed increased urinary excretion of PEA, suggesting the accumulation of substrates for TNSALP in the body. He exhibited delayed

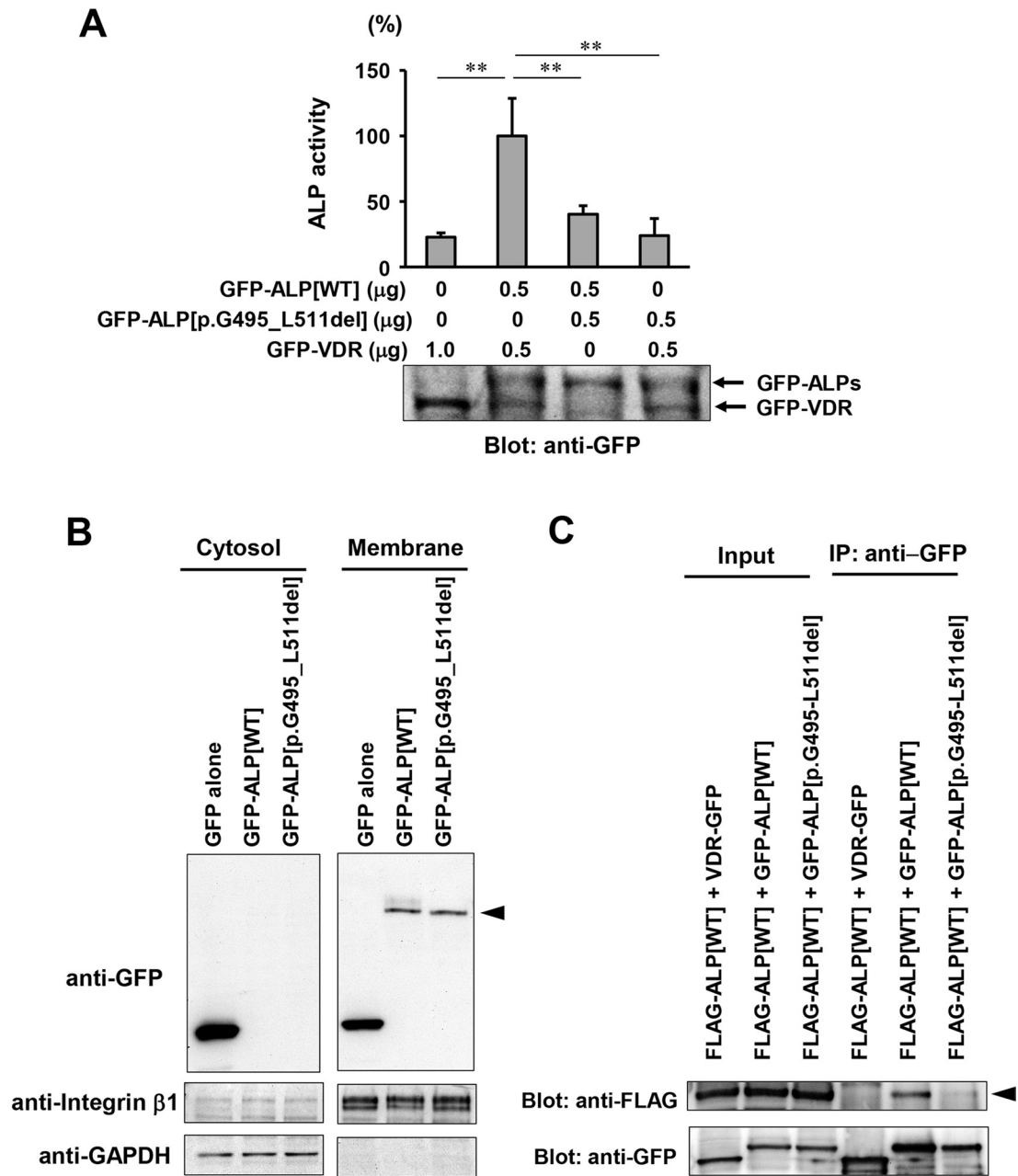


Fig. 3. Characterization of the TNSALP[p.Gly495_Leu511del] variant. (A) Loss of enzymatic activity and the dominant-negative effect of TNSALP[p.Gly495_Leu511del]. The indicated amounts of expression plasmids encoding GFP-tagged TNSALP[WT] and [p.Gly495_Leu511del] were transfected into COS7 cells. We used an expression plasmid encoding GFP-tagged vitamin D receptor (GFP-VDR) as a mock plasmid. Three days later, the enzymatic activity in the cell lysates was determined and was normalized based on the intensity of the signals in western blotting using aliquots of the lysates and probed using anti-GFP antibodies. The enzymatic activity in the cells transfected with GFP-TNSALP[WT] and GFP-VDR was designated as 100%. Data are shown as the mean ± SD (N = 3). ** $p < 0.01$ using one-way ANOVA with the Tukey-Kramer method for post hoc tests. (B) Localization of TNSALP[WT] and TNSALP[p.Gly495_Leu511del] to the plasma membrane. The cytosolic and membrane fractions of COS7 cells expressing GFP alone, GFP-TNSALP[WT], or GFP-TNSALP[p.Gly495_Leu511del] were harvested and subjected to western blotting using the indicated primary antibodies. The arrowhead indicates the position of GFP-TNSALPs. (C) Reduced dimer formation and/or stability between TNSALP[Gly495_511del] and TNSALP[WT]. COS7 cells were transfected with a plasmid encoding FLAG-tagged TNSALP[WT] together with those for VDR-GFP, GFP-TNSALP[WT], or GFP-TNSALP[p.Gly495_Leu511del]. The cell lysates were then subjected to co-immunoprecipitation using anti-GFP antibodies, followed by western blotting using anti-FLAG and anti-GFP antibodies. The arrowhead indicates the position of FLAG-TNSALP[WT].

ossification of the carpal bones, radiolucency of the finger bones, extremely low BMD, and short stature, which may be HPP-associated symptoms. We also identified a novel heterozygous 51-bp in-frame deletion in the *ALPL* gene in this patient, and *in vitro* transfection experiments suggested the loss of enzymatic activity and a dominant-negative effect of the resultant variant TNSALP[p.Gly495_Leu511del] protein (**Fig. 2A**). Based on these findings, we diagnosed the patient as having autosomal dominant HPP.

The human *ALPL* gene consists of 12 exons, including coding exons 2–12 (5). The 51-bp region deleted in the current patient is located in exon 12. The TNSALP protein is anchored to the plasma membrane through a covalent linkage to glycosylphosphatidylinositol (GPI). The GPI-anchoring signal of TNSALP corresponds to amino acids Leu506 to Phe524 (9), which partly overlaps the deleted region in the TNSALP[p.Gly495_Leu511del] variant. However, our western blotting results from the membrane fractions demonstrated that the TNSALP[p.Gly495_Leu511del] variant localized to the plasma membrane, similar to TNSALP[WT] (**Fig. 2B**).

Although both the TNSALP[p.Gly495_Leu511del] variant and TNSALP[WT] were found to be localized to the plasma membrane, it was suggested that the heterodimer formation/stability of the TNSALP[p.Gly495_Leu511del] variant with the TNSALP[WT] was markedly reduced compared to the homodimer formation/stability between two TNSALP[WT] proteins (**Fig. 2C**). The deleted region in the TNSALP[p.Gly495_Leu511del] variant did not overlap with, but was close to, the putative homodimeric interface of the TNSALP[WT] protein (10). Hence, the conformational change due to the 17-amino acid deletion might have impaired the dimer formation/stability. More than 20 *ALPL* variants have been shown to have

dominant-negative effects in *in vitro* experiments, and many of these dominant-negative variants are located in the homodimer interface (11). We speculate that impaired dimer formation/stability might be one of the mechanisms for the dominant-negative effects of some *ALPL* variants.

The father of the patient in the present case had a normal height and did not currently show any symptoms of HPP, although he shared the same heterozygous *ALPL* variant with the patient and a history of fractures. While the penetrance of recessive HPP is assumed to be complete, incomplete penetrance and variable expressivity are possible in autosomal dominant HPP (12). We should keep in mind that the father may manifest some HPP-related symptoms later in his life.

In conclusion, we described a case of childhood HPP caused by a heterozygous 51-bp in-frame deletion of the *ALPL* gene. His initial chief complaint was short stature. *In vitro* studies confirmed the loss of enzymatic activity of the identified TNSALP[p.Gly495_Leu511del] variant and also revealed its dominant-negative effect. TNSALP[p.Gly495_Leu511del] exhibited a decreased binding to TNSALP[WT], which suggested that impaired dimer formation/stability might underlie the dominant-negative effects of this TNSALP variant.

Conflict of interests: Toshimi Michigami received lecture fees from Alexion Pharmaceuticals, Inc.

Acknowledgements

This work was supported by a grant from Research on Rare and Intractable Diseases, Health, Labour and Welfare Sciences Research Grants 22FC1012 (Principal Investigator, Takuo Kubota).

References

1. Whyte MP. Hypophosphatasia - aetiology, nosology, pathogenesis, diagnosis and treatment. *Nat Rev Endocrinol* 2016;12: 233–46. [[Medline](#)] [[CrossRef](#)]
2. Michigami T, Tachikawa K, Yamazaki M, Kawai M, Kubota T, Ozono K. Hypophosphatasia in Japan: *ALPL* mutation analysis in 98 unrelated patients. *Calcif Tissue Int* 2020;106: 221–31. [[Medline](#)] [[CrossRef](#)]
3. Michigami T, Ohata Y, Fujiwara M, Mochizuki H, Adachi M, Kitaoka T, *et al.* Clinical practice guidelines for hypophosphatasia. *Clin Pediatr Endocrinol* 2020;29: 9–24. [[Medline](#)] [[CrossRef](#)]
4. Imbard A, Alberti C, Armoogum-Boizeau P, Ottolenghi C, Jossierand E, Rigal O, *et al.* Phosphoethanolamine normal range in pediatric urines for hypophosphatasia screening. *Clin Chem Lab Med* 2012;50: 2231–3. [[Medline](#)] [[CrossRef](#)]
5. Henthorn PS, Raducha M, Fedde KN, Lafferty MA, Whyte MP. Different missense mutations at the tissue-nonspecific alkaline phosphatase gene locus in autosomal recessively inherited forms of mild and severe hypophosphatasia. *Proc Natl Acad Sci USA* 1992;89: 9924–8. [[Medline](#)] [[CrossRef](#)]
6. Cai G, Michigami T, Yamamoto T, Yasui N, Satomura K, Yamagata M, *et al.* Analysis of localization of mutated tissue-nonspecific alkaline phosphatase proteins associated with neonatal hypophosphatasia using green fluorescent protein chimera. *J Clin Endocrinol Metab* 1998;83: 3936–42. [[Medline](#)]
7. Yamazaki M, Kawai M, Kinoshita S, Tachikawa K, Nakanishi T, Ozono K, *et al.* Clonal osteoblastic cell lines with CRISPR/Cas9-mediated ablation of Pit1 or Pit2 show enhanced mineralization despite reduced osteogenic gene expression. *Bone* 2021;151: 116036. [[Medline](#)] [[CrossRef](#)]
8. Millán JL, Whyte MP. Alkaline phosphatase and hypophosphatasia. *Calcif Tissue Int* 2016;98: 398–416. [[Medline](#)] [[CrossRef](#)]
9. Nishioka T, Tomatsu S, Gutierrez MA, Miyamoto K, Trandafirescu GG, Lopez PL, *et al.* Enhancement of drug delivery to bone: characterization of human tissue-nonspecific alkaline phosphatase tagged with an acidic oligopeptide. *Mol Genet*

- Metab 2006;88: 244–55. [\[Medline\]](#) [\[CrossRef\]](#)
10. Silvent J, Gasse B, Mornet E, Sire JY. Molecular evolution of the tissue-nonspecific alkaline phosphatase allows prediction and validation of missense mutations responsible for hypophosphatasia. *J Biol Chem* 2014;289: 24168–79. [\[Medline\]](#) [\[CrossRef\]](#)
 11. Del Angel G, Reynders J, Negron C, Steinbrecher T, Mornet E. Large-scale in vitro functional testing and novel variant scoring via protein modeling provide insights into alkaline phosphatase activity in hypophosphatasia. *Hum Mutat* 2020;41: 1250–62. [\[Medline\]](#) [\[CrossRef\]](#)
 12. Mornet E. Hypophosphatasia. *Metabolism* 2018;82: 142–55. [\[Medline\]](#) [\[CrossRef\]](#)